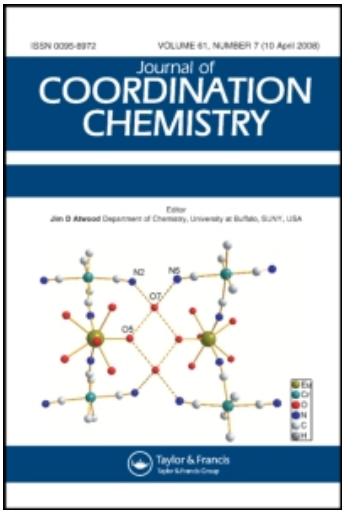


**Journal of Coordination Chemistry**
Publication details, including instructions for authors and subscription information:
http://www.informaworld.com/smpp/title~content=t713455674

# A new organic-inorganic hybrid polyoxoniobate based on Lindqvist-type anion and nickel complex

Guo Chen[a]; Pengtao Ma[a]; Jingping Wang[a]; Jingyang Niu[a]
[a] Institute of Molecular and Crystal Engineering, College of Chemistry and Chemical Engineering, Henan University, Kaifeng, Henan 475004, P.R. China

First published on: 29 September 2010

**To cite this Article** Chen, Guo , Ma, Pengtao , Wang, Jingping and Niu, Jingyang(2010) 'A new organic-inorganic hybrid polyoxoniobate based on Lindqvist-type anion and nickel complex', Journal of Coordination Chemistry, 63: 21, 3753 — 3763, First published on: 29 September 2010 (iFirst)
**To link to this Article: DOI:** 10.1080/00958972.2010.520709
**URL:** http://dx.doi.org/10.1080/00958972.2010.520709

*Journal of Coordination Chemistry*
Vol. 63, No. 21, 10 November 2010, 3753–3763



# A new organic–inorganic hybrid polyoxoniobate based on Lindqvist-type anion and nickel complex

GUO CHEN, PENGTAO MA, JINGPING WANG and JINGYANG NIU*

Institute of Molecular and Crystal Engineering,
College of Chemistry and Chemical Engineering,
Henan University, Kaifeng, Henan 475004, P.R. China

(*Received 11 May 2010; in final form 23 July 2010*)



A new organic–inorganic hybrid polyoxoniobate $(H_2en)_2[Ni(en)_3][H_2Nb_6O_{19}]\cdot 5.5H_2O$ (**1**) (en = ethylenediamine) has been synthesized by the diffusion method and structurally characterized by elemental analyses, infrared spectrum, ultraviolet (UV) spectroscopy, X-ray photoelectron spectroscopy (XPS), X-ray powder diffraction, thermogravimetric (TG) analysis, and single-crystal X-ray diffraction. Crystal structure analysis reveals that **1** exhibits a 3-D supramolecular architecture constructed from Lindqvist-type $[H_2Nb_6O_{19}]^{6-}$ polyoxoanions and $[Ni(en)_3]^{2+}$ *via* hydrogen-bonding interactions. The XPS measurement indicates that the oxidation state of Ni is +2. TG curve of **1** exhibits two steps of weight loss. *In situ* UV spectra display that **1** can exist in large pH range in aqueous solution.

*Keywords*: Polyoxoniobate; Organic–inorganic hybrid; Lindqvist-type; Hydrogen bond; Crystal structure

## 1. Introduction

Polyoxometalate (POM) chemistry has attracted increasing interest for their variety of architectures and properties and potential applications in catalysis, magnetism, material science, and medicinal chemistry [1–4].

Polyoxoniobates, as an important subclass in POM chemistry, have made considerable progress in recent years and some polyoxoniobate clusters with unexpected structures and properties have been reported. In 1969, Flynn and Stucky [5, 6] reported two sandwich-type hexaniobate Lindqvist dimers $[Mn(Nb_6O_{19})_2]^{12-}$ and $[Ni(Nb_6O_{19})_2]^{12-}$. In 1977, Graeber and Morosin [7] obtained the decaniobate $[Nb_{10}O_{28}]^{6-}$ cluster in nonaqueous solvent, which can be described as a hexaniobate unit $[Nb_6O_{19}]^{8-}$ capped by a tetraniobate $[Nb_4O_9]^{2+}$. Subsequently, Yamase *et al.* [8–10] discovered a family of lanthanide-containing polyoxoniobates $\{[Ln_3O(OH)_3(H_2O)_3]_2Al_2(Nb_6O_{19})_5\}^{26-}$ (Ln = $Eu^{III}$, $Er^{III}$, $Lu^{III}$). Pope *et al.* [11] synthesized two tricarbonyl metal derivatives of hexaniobates

*Corresponding author. Email: jyniu@henu.edu.cn

*Journal of Coordination Chemistry*
ISSN 0095-8972 print/ISSN 1029-0389 online © 2010 Taylor & Francis
DOI: 10.1080/00958972.2010.520709

$[Nb_6O_{19}\{M(CO)_3\}_n]^{(8-n)-}$ ($M = Re^I$, $Mn^I$) in 2001. In 2002–2008, Nyman *et al.* [12–16] prepared several Keggin-type heteropolyniobates, such as $[XNb_{12}O_{40}]^{y-}$ ($X = Si^{IV}, Ge^{IV}, P^V$; $y = 15, 16$) and their derivatives $[H_2Si_4Nb_{16}O_{56}]^{14-}$ and $[(PO_2)_3PNb_9O_{34}]^{15-}$ as well as a large isopolyniobate $[Nb_{24}O_{72}H_9]^{15-}$ built by three $[Nb_7O_{22}]^{9-}$ fragments linked by three $NbO_6$ octahedra [17]. In 2006, Maekawa *et al.* [18] reported an icositetraniobate cluster $[Nb_{20}O_{54}]^{8-}$ constructed from two decaniobate $[Nb_{10}O_{28}]^{6-}$ units by sharing two terminal oxygens. In 2007, our group reported four giant polyniobates constructed from $[Nb_7O_{22}]^{9-}$ units [19]. In 2010, Cronin *et al.* [20] reported two high-nuclearity isopolyoxoniobates clusters $[HNb_{27}O_{76}]^{16-}$ and $[HNb_{31}O_{93}(CO_3)]^{23-}$. More recently, our group addressed two copper-undecaniobates $\{[Cu(H_2O)L]_2[CuNb_{11}O_{35}H_4]\}^{5-}$ (L = 1,10-phenanthroline, 2,2′-bipyridine) consisting of plenary and monolacunary Lindqvist-type isopolyniobate fragments [21].

Recently, organic–inorganic hybrid polyoxoniobates received attention and some transition metal complex-containing polyoxoniobates have been reported [17, 19, 21–26], for example, $[Cu(en)_2(H_2O)_2]_2[(Nb_6O_{19}H_2)Cu(en)_2] \cdot 14H_2O$ [22], $\{[M(2,2'\text{-bipy})_2]_3[Nb_{10}O_{28}] \cdot mH_2O\}_n$ ($M = Co^{II}, Zn^{II}$) [23], $\{Nb_6O_{19}[Cu(2,2'\text{-bipy})]_2[Cu(2,2'\text{-bipy})_2]_2\} \cdot 19H_2O$ [24], $Na[Cu(1,3\text{-dap})_2]_3[HNb_6O_{19}] \cdot 3H_2O$ [25], and $K_8Na_2\{[Cu(en)(H_2O)]_2[HNb_6O_{19}]_2\} \cdot 25H_2O$ [26]. Obviously, most are Cu-complex-containing polyoxoniobates, with polyoxoniobates decorated by other transition metal complexes being less exploited, especially Ni-complex-containing polyoxoniobates. To date, only two polyoxoniobates decorated by nickel complexes $[Ni(taci)_2]_2\{trans\text{-}[Nb_6O_{19}][Ni(taci)]_2\} \cdot 26H_2O$ and $[Na(H_2O)_6]_2\{cis\text{-}[H_2Nb_6O_{19}][Ni(taci)]_2\} \cdot 18H_2O$ have been reported [27], providing an opportunity for exploring and designing Ni-containing polyoxoniobates by introducing nickel ion and organic ligand into the hexaniobate system. Fortunately, a new Ni-complex-containing polyoxoniobate $(H_2en)_2[Ni(en)_3][H_2Nb_6O_{19}] \cdot 5.5H_2O$ (**1**) has been isolated using the diffusion strategy. To the best of our knowledge, **1** represents the first organic–inorganic hybrid polyoxoniobate based on $[H_2Nb_6O_{19}]^{6-}$ and $[Ni(en)_3]^{2+}$.



## 2. Experimental

### 2.1. *Materials and physical measurements*

$K_7HNb_6O_{19} \cdot 13H_2O$ was prepared according to the literature [28] and identified by infrared (IR) spectrum. All other reagents were purchased from commercial sources and used without purification.

C, H, and N elemental analyses were performed on a Perkin-Elmer 2400-II CHNS/O analyzer. The IR spectrum was recorded on a Nicolet FT-IR 360 spectrometer using KBr pellets from 400 to 4000 $cm^{-1}$. X-ray photoelectron spectroscopy (XPS) analysis was performed on an Axis Ultra (Kratos, UK) photoelectron spectroscope using monochromatic Al-Kα (1486.7 eV) radiation. X-ray powder diffraction (XRPD) measurement was performed on a Philips X'Pert-MPD instrument with Cu-Kα radiation ($\lambda = 1.54056$ Å) in the angular range $2\theta = 10$–$45^\circ$ at 293 K. Thermogravimetric (TG) measurement was carried out on a Mettler-Toledo TGA/SDTA851$^e$ thermal analyzer in flowing $N_2$ between 25°C and 800°C at a heating rate of 10°C $min^{-1}$. Ultraviolet (UV) spectra were recorded with a HITACHI U-4100 UV-Vis-NIR spectrometer (distilled water as solvent) from 400 to 190 nm.

### 2.2. *Preparation of $(H_2en)_2[Ni(en)_3][H_2Nb_6O_{19}] \cdot 5.5H_2O$ (1)*

Ethylenediamine (en) (10 mL) was added to a stirred solution of $NiCl_2 \cdot 6H_2O$ (0.582 g, 2.0 mmol) dissolved in 20 mL water. Then the pink solution was added dropwise to a stirred aqueous solution (50 mL) containing $K_7HNb_6O_{19} \cdot 13H_2O$ (0.690 g, 0.500 mmol). Finally, the resulting mixture was kept at 70°C with stirring for 8 h, filtered, and then transferred to a straight glass tube. Acetonitrile was carefully layered onto the resulting light-purple solution. Diffusion between the two phases over 3 weeks produced block-shaped light purple single crystals of **1**. Yield: 33% based on $K_7HNb_6O_{19} \cdot 13H_2O$. Anal. Found: (Calcd) (%): C, 8.92 (9.06); H, 4.26 (4.33); N, 10.68 (10.57).

### 2.3. *X-ray structure determination*

Intensity data were collected on a Bruker APEX-II CCD diffractometer with Mo-Kα monochromated radiation (λ = 0.71073 Å) at 273(2) K. The structure was solved by direct methods and refined by full-matrix least-squares on $F^2$ using the SHELXL-97 software [29]. All the non-hydrogen atoms were refined anisotropically. The organic hydrogens were generated geometrically. A summary of crystal data and structure refinement for **1** is provided in table 1. Selected bond lengths and angles of **1** are listed in table 2.



## 3. Results and discussion

### 3.1. *Synthesis*

Compound **1** was synthesized by the reaction of $K_7HNb_6O_{19} \cdot 13H_2O$, $NiCl_2 \cdot 6H_2O$, en, and $H_2O$ using the diffusion strategy. During the synthetic processes, the diffusion approach played a crucial role. Diffusion technique is extensively used and provides an effective method for crystal growth in supramolecule chemistry and coordination chemistry [30, 31], but is rarely utilized in synthesizing POMs [32], especially for polyoxoniobates. Currently, our lab is making great efforts to introduce the diffusion technique to polyoxoniobate chemistry [21, 26]. A large number of experimental results indicate that good quality crystals of **1** were not obtained by hydrothermal technique or evaporation solvent method at atmospheric pressure.

### 3.2. *Crystal structure of 1*

The experimental XRPD pattern of the bulk product of **1** is in good agreement with the simulated XRPD pattern based on the result from single-crystal X-ray diffraction, indicating phase purity of the sample (figure 1). Single crystal X-ray diffraction analysis reveals that **1** consists of one biprotonated Lindqvist-type polyoxoanion $[H_2Nb_6O_{19}]^{6-}$, one $[Ni(en)_3]^{2+}$, two biprotonated $(H_2en)^{2+}$, and 5.5 lattice water molecules (figure 2). The biprotonated polyoxoanion $[H_2Nb_6O_{19}]^{6-}$ retains the well-known Lindqvist structure [33], which is fused together with six edge-shared $NbO_6$ octahedra. In the crystal structure of **1**, the niobium–oxygen distances, as expected, are divided into three groups: the niobium–terminal oxygens, Nb–$O_t$, within the range of 1.772(4)–1.780(5) Å

Table 1. Crystallographic data and structure refinement for **1**.

| | |
|---|---|
| Empirical formula | $C_{10}H_{57}N_{10}Nb_6NiO_{24.50}$ |
| Formula weight | 1325.74 |
| Temperature (K) | 273(2) |
| Wavelength λ (Å) | 0.71073 |
| Crystal system | Orthorhombic |
| Space group | *Pca2(1)* |
| Unit cell dimensions (Å, °) | |
| *a* | 20.672(10) |
| *b* | 12.742(6) |
| *c* | 15.518(8) |
| α | 90.00 |
| β | 90.00 |
| γ | 90.00 |
| Volume (Å$^3$), *Z* | 4088(3), 4 |
| Crystal size (mm$^3$) | $0.15 \times 0.14 \times 0.13$ |
| Calculated density (g cm$^{-3}$) | 2.136 |
| Absorption coefficient (mm$^{-1}$) | 2.161 |
| Reflections collected | 28,818 |
| Independent reflections | 7175 [$R_{(int)} = 0.0179$] |
| Data/restraints/parameters | 7175/31/470 |
| Goodness-of-fit on $F^2$ | 1.023 |
| Completeness | 99.6% |
| *F*(000) | 2584 |
| Index range | $-24 \le h \le 24$; $-15 \le k \le 15$; $-18 \le l \le 18$ |
| Final *R* indices [$I > 2\sigma(I)$] | $R_1 = 0.0301$, $wR_2 = 0.0887$ |
| *R* indices (all data) | $R_1 = 0.0310$, $wR_2 = 0.0896$ |
| Largest difference peak and hole (e Å$^{-3}$) | 1.887 and −1.524 |

Table 2. Selected bond lengths (Å) and angles (°) for **1**.

| | | | |
|---|---|---|---|
| Nb1–O1 | 1.773(4) | Nb2–O2 | 1.772(4) |
| Nb3–O3 | 1.777(4) | Nb4–O4 | 1.777(5) |
| Nb5–O5 | 1.772(5) | Nb6–O6 | 1.780(5) |
| Nb6–O17 | 2.174(4) | Nb3–O8 | 1.917(4) |
| Nb5–O19 | 2.454(4) | Nb3–O19 | 2.354(4) |
| Ni1–N1 | 2.115(7) | Ni1–N2 | 2.131(7) |
| Ni1–N3 | 2.101(7) | Ni1–N6 | 2.122(7) |
| Ni1–N4 | 2.154(9) | Ni1–N5 | 2.073(7) |
| N5–Ni1–N1 | 97.1(3) | N3–Ni1–N4 | 80.6(3) |
| N6–Ni1–N4 | 90.1(3) | N5–Ni1–N2 | 94.0(3) |
| O1–Nb1–O9 | 104.6(2) | O1–Nb1–O8 | 101.6(2) |
| O14–Nb2–O19 | 80.91(16) | O11–Nb2–O19 | 76.00(15) |
| O3–Nb3–O11 | 97.9(2) | O3–Nb3–O12 | 104.7(2) |
| O9–Nb4–O13 | 89.40(19) | O16–Nb4–O12 | 85.41(18) |
| O5–Nb5–O14 | 102.0(2) | O5–Nb5–O18 | 102.6(2) |
| O18–Nb6–O19 | 81.11(16) | O17–Nb6–O19 | 75.82(15) |

(av. 1.775 Å), bridging oxygens, Nb–$O_b$, 1.917(4)–2.174(4) Å (av. 2.013 Å), and central oxygen bridging, Nb–$O_c$, 2.354(4)–2.454(4) Å (av. 2.396 Å). The O–Nb–O bond angles vary from 75.03(16)° to 104.7(2)°, indicating that $NbO_6$ octahedra are slightly distorted. The geometric parameters are in good agreement with those reported previously [11]. Bond valence sum (BVS) [34] calculations gave values of 1.42–1.46 for all terminal oxygens in $[Nb_6O_{19}]^{8-}$ anion, suggesting that two of the terminal oxygens in the $[Nb_6O_{19}]^{8-}$ cluster can be monoprotonated [17, 19]. Although the two protons cannot

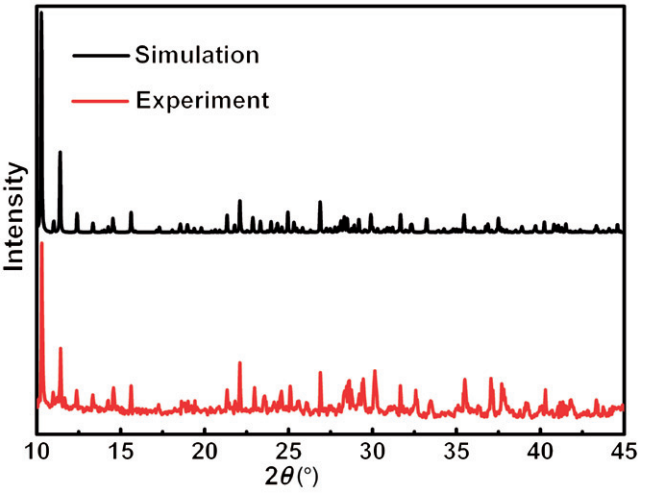


Figure 1. Comparison of the simulated and experimental XRPD patterns of **1**.



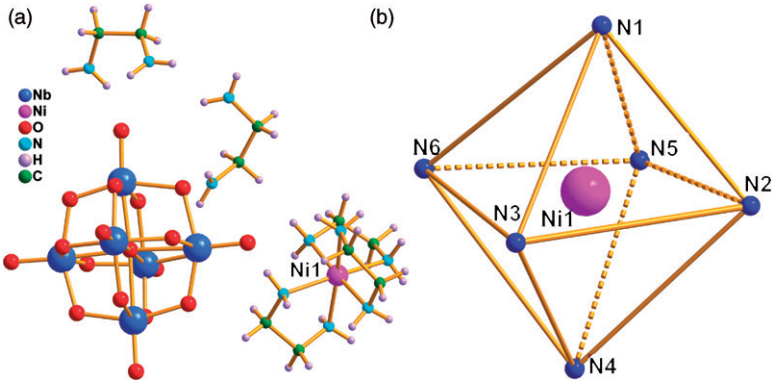


Figure 2. (a) The molecular structure unit of **1** (the lattice water molecules are omitted for clarity) and (b) view of coordination geometry of $Ni^{2+}$.

be accurately located by X-ray diffraction and BVS calculations, the protons must be localized or delocalized in the $[Nb_6O_{19}]^{8-}$ unit.

Besides the Lindqvist polyoxoanion $[H_2Nb_6O_{19}]^{6-}$, there are a discrete $[Ni(en)_3]^{2+}$ and two biprotonated $(H_2en)^{2+}$ acting as counter cations. In $[Ni(en)_3]^{2+}$, the $Ni^{2+}$ has six nitrogens from three en forming a distorted $\{NiN_6\}$ octahedron with Ni–N bond lengths of 2.073(7)–2.154(9) Å (av. 2.116 Å). BVS calculation of the nickel is 1.73, indicating the oxidation state of nickel is +2, consistent with six-coordinate geometry and the requirements of charge balance. The presence of $Ni^{2+}$ in **1** is further identified by XPS (see below). Additionally, according to the reaction environment, two en molecules should be biprotonated [17, 35], agreeing with the molecular formula of $(H_2en)_2[Ni(en)_3][H_2Nb_6O_{19}] \cdot 5.5\ H_2O$.

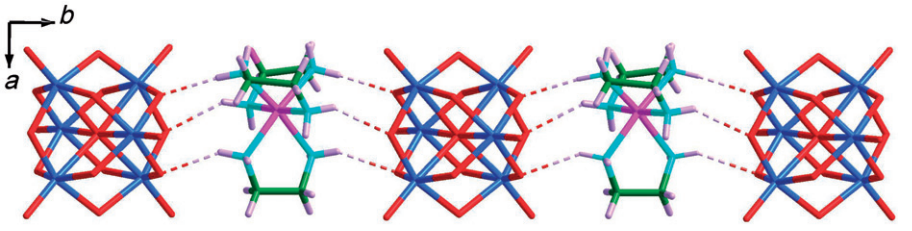


Figure 3. The 1-D infinite chain formed by $[Ni(en)_3]^{2+}$ and $[H_2Nb_6O_{19}]^{6-}$ connected alternately through N–H···$O_b$ hydrogen bonds.

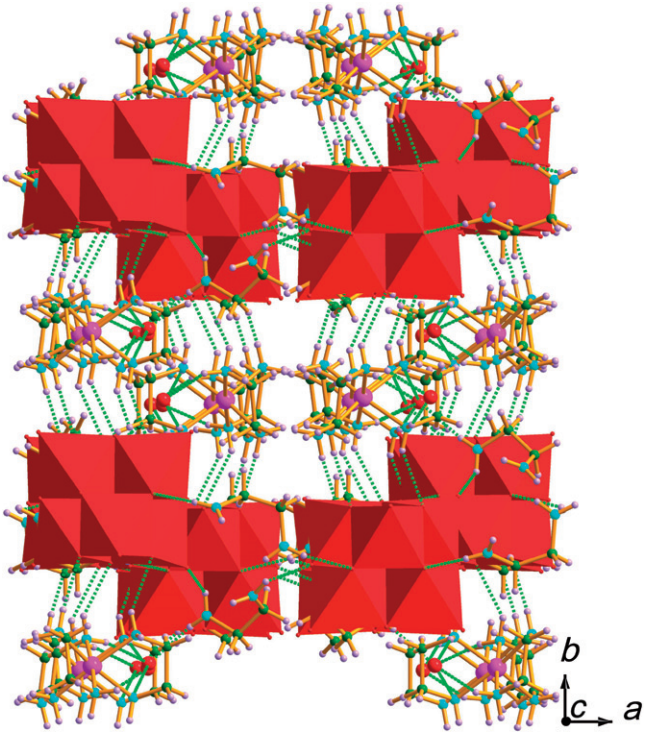


Figure 4. The 3-D supramolecular architecture of **1** formed through N–H···$O_{b,t}$ (N–H···$O_W$) hydrogen bond interactions. Color code: $NbO_6$, red; Ni, pink; hydrogen bond, green.

In the structure of **1**, the isolated $[Ni(en)_3]^{2+}$ cations and $[H_2Nb_6O_{19}]^{6-}$ polyoxoanions connect alternately through N–H···$O_b$ hydrogen-bonding interactions, forming an infinite 1-D chain along the *c*-axis with N···$O_b$ distances in the range 3.030–3.082 Å (figure 3). The 1-D chain is further extended into a 3-D supramolecular architecture *via* N–H···$O_{b,t}$ and N–H···$O_W$ hydrogen bonds between $(H_2en)^{2+}$, $[H_2Nb_6O_{19}]^{6-}$, $O_{3W}$, and $O_{4W}$, with the corresponding N···$O_{b,t}$ distances: 2.691–3.074 Å, N···$O_W$ distances: 2.884–3.474 Å (figure 4). Obviously, these hydrogen-bonding interactions strengthened the stability of the 3-D supramolecular structure of **1**. The details of the hydrogen bonds are listed in table 3.

Table 3. Hydrogen bond lengths (Å) and angles (°) of **1**.

| D–H···A | *d*(D–H) | *d*(H···A) | *d*(D···A) | ∠D–H···A |
|---|---|---|---|---|
| N1–H1D···O9 | 0.900 | 2.152 | 3.030 | 164.92 |
| N2–H2C···O3W | 0.900 | 2.291 | 3.129 | 154.83 |
| N2–H2D···O14 | 0.900 | 2.288 | 3.073 | 145.65 |
| N3–H3C···O3W | 0.900 | 2.415 | 3.273 | 159.61 |
| N3–H3D···O8 | 0.900 | 2.311 | 3.073 | 142.24 |
| N4–H4C···O4W | 0.900 | 2.652 | 3.474 | 152.35 |
| N4–H4D···O15 | 0.900 | 2.318 | 3.082 | 142.57 |
| N5–H5D···O18 | 0.900 | 2.173 | 3.046 | 163.18 |
| N6–H6C···O4W | 0.900 | 2.466 | 3.343 | 164.95 |
| N6–H6D···O12 | 0.900 | 2.296 | 3.082 | 145.75 |
| N7–H7D···O13 | 0.860 | 1.912 | 2.691 | 150.04 |
| N8–H8C···O3 | 0.860 | 2.130 | 2.702 | 123.57 |
| N8–H8D···O4W | 0.860 | 2.095 | 2.884 | 152.16 |
| N9–H9D···O10 | 0.860 | 2.110 | 2.820 | 139.53 |
| N10–H10C···O16 | 0.860 | 2.255 | 3.074 | 159.01 |
| N10–H10C···O12 | 0.860 | 2.339 | 2.894 | 122.53 |
| N10–H10C···O17 | 0.860 | 2.445 | 3.007 | 123.50 |
| N10–H10D···O7 | 0.860 | 1.867 | 2.693 | 160.45 |



### 3.3. *IR and XPS spectra*

The IR spectrum of **1** (Supplementary material) exhibits five characteristic vibrations resulting from $[H_2Nb_6O_{19}]^{6-}$. The peak at 855 $cm^{-1}$ is attributed to terminal Nb–$O_t$ vibration, as well as peaks at 741, 646, 535, and 407 $cm^{-1}$ assigned to bridging Nb–$O_b$–Nb vibration. Compared with the IR spectrum of the precursor $K_7HNb_6O_{19}\cdot 13H_2O$ (852, 777, 669, 519, 413 $cm^{-1}$) [11], the vibration bands are slightly shifted, partially effected by hydrogen-bonding interactions between the $[H_2Nb_6O_{19}]^{6-}$ and nickel complex. Additionally, the –OH and $-NH_2$ stretching bands are observed at 3460–3420 and 3350–3230 $cm^{-1}$, respectively. The bending vibration bands of $-NH_2$, $-CH_2$, and C–N groups appear at 1642–1580, 1518–1460, and 1032 $cm^{-1}$, respectively [36]. The occurrence of these absorptions is assigned to the presence of en, which conforms to the results of single-crystal structural analyses.

Although the oxidation state of nickel in **1** has been determined as +2 by means of theoretical BVS calculations, in order to further confirm the oxidation state of nickel atom by means of experimental technique, the XPS measurement of **1** is performed (figure 5). The XPS spectrum exhibits two peaks at 854.6 and 872.5 eV, which can be attributed to $Ni^{2+}$ ($2p_{3/2}$) and $Ni^{2+}$ ($2p_{1/2}$), respectively. These values are in agreement with the values reported in the literature [37].

### 3.4. *TG analysis*

The TG curve of **1** exhibits two steps of weight loss (Supplementary material), giving a total loss of 32.35% (Calcd 31.80%) in the range of 25–800°C. The first weight loss of 7.77% at 25–126°C is ascribed to the loss of 5.5 lattice water molecules (Calcd 7.47%); the second weight loss of 24.58% at 127–750°C is assigned to the removal of two isolated $(H_2en)^{2+}$ cations, three en ligands, and dehydration of two protons (Calcd 24.33%).

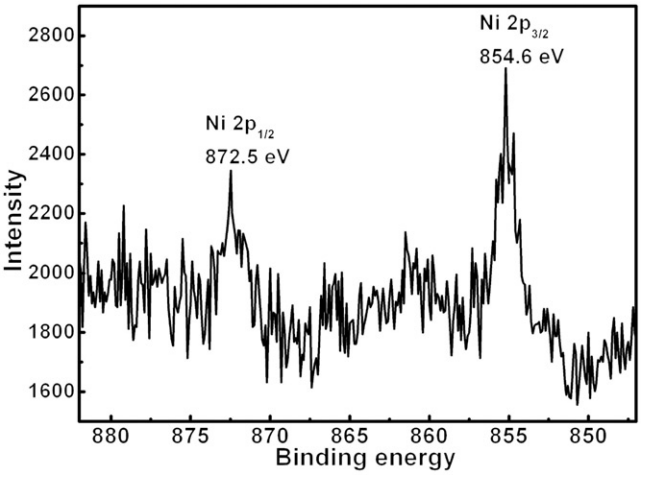


Figure 5. X-ray photoelectron spectrum of **1**.



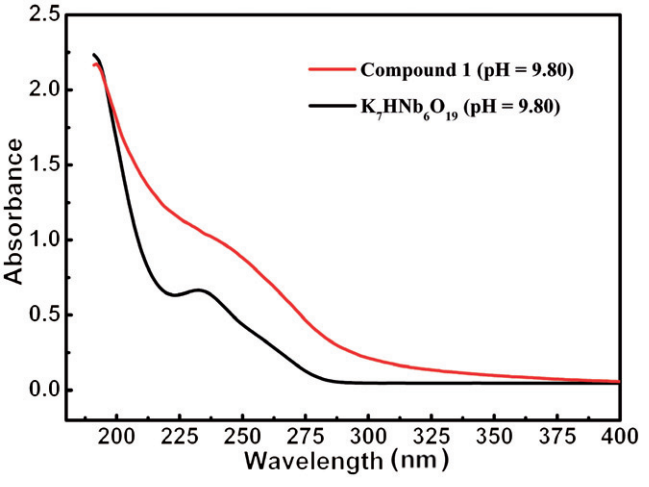


Figure 6. Comparison of the UV spectra of **1** and $K_7HNb_6O_{19}$ in aqueous solution ($1 \times 10^{-5}$ mol $L^{-1}$, pH = 9.80).

### 3.5. *UV spectra and the stability measurements*

In order to study the solution optical property of **1**, its UV spectrum is performed in aqueous solution (at pH = 9.80) (figure 6). The UV spectrum displays one strong absorption centered at 193 nm and one wide shoulder absorption centered at *ca* 242 nm in the region of 400–190 nm, which are assigned to the O → Nb charge transfer transitions [21, 26]. Compared with the UV spectra of the precursor $K_7HNb_6O_{19} \cdot 13H_2O$ (*ca* 192 and 233 nm), the absorption bands are slightly red shifted. The red-shift phenomena of the O → Nb charge transfer absorption bands may be related to the interactions between polyoxoanions and metal–organic cations (mainly including static electronic interaction and hydrogen bonding interactions).

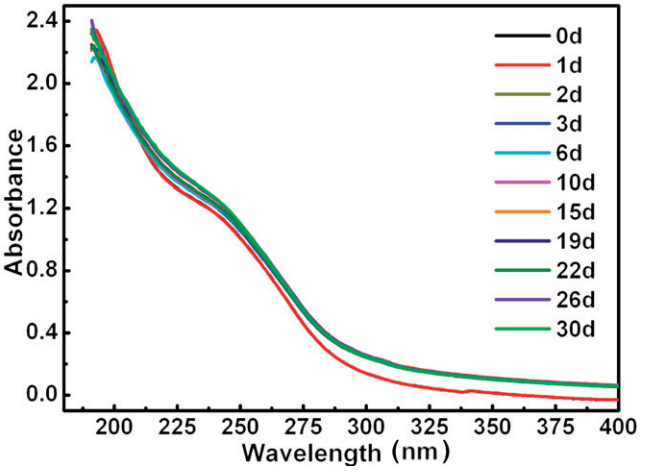


Figure 7. Aging of the solution of **1** detected by the *in situ* UV spectra.



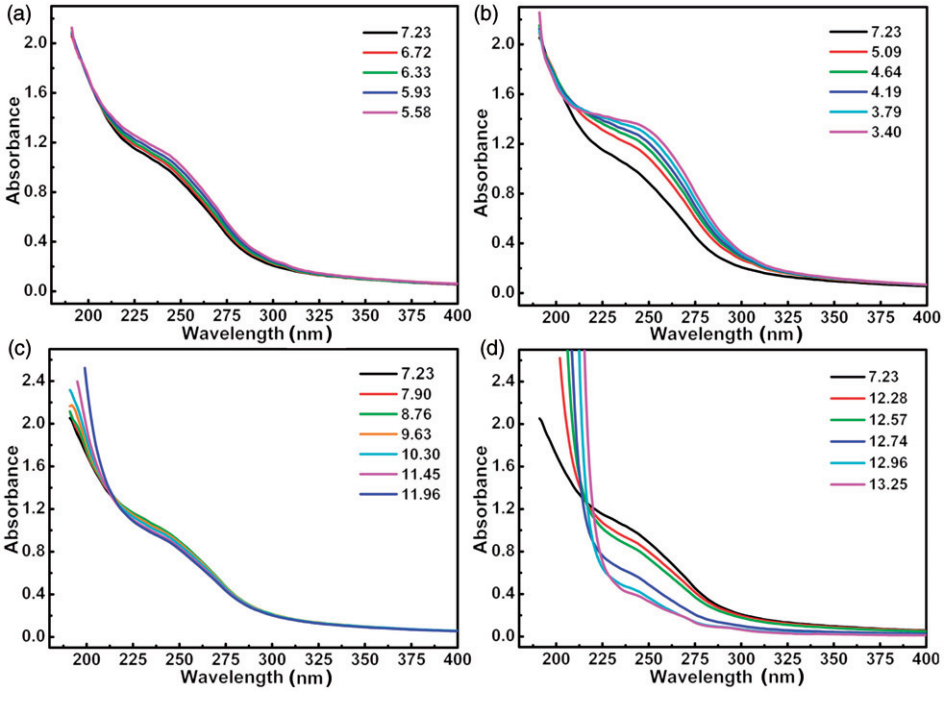


Figure 8. (a) and (b) The UV spectral evolution in the acidic direction; (c) and /(d) the UV spectral evolution in the alkaline direction. The pH value that **1** is dissolved in water ($1 \times 10^{-5}$ mol $L^{-1}$) is 7.23. The pH values are adjusted using dilute HCl or NaOH solutions.

To investigate the stability of **1** in solution, its aqueous system is studied by *in situ* UV spectra (figure 7). The systematic results reveal that **1** ($1 \times 10^{-5}$ mol $L^{-1}$) does not dissociate in aqueous solution, but remains stable at least 30 days at ambient temperature. Polyoxoniobates are commonly sensitive to pH of the studied media, so

the influences of the pH value on the stability of **1** in the aqueous solution have been probed by UV spectra (figure 8). Adjusting using HCl or NaOH solution allows us to monitor if **1** can be stable in aqueous solution at pH 5.5–12. As shown in figure 8(a) and (b), when the solution acidity of **1** gradually becomes stronger, the absorption band at *ca* 193 nm is pushed to the near-UV region, the absorption band at *ca* 242 nm is gradually red-shifted and disappears (pH < 5.5); we observed a large amount of precipitate from the solution of **1** when the pH is lower than 5.5. The increase of precipitates and disappearance of the absorption band at *ca* 193 and 242 nm illustrate that **1** begins to slowly decompose, transformed to hydrous niobium oxide $Nb_2O_5 \cdot xH_2O$ and $[Ni(en)_3]Cl_2$ upon the addition of HCl solution. In contrast, when the solution alkalinity of **1** becomes stronger (figure 8c and d), absorptions at *ca* 242 nm are gradually blue-shifted to 233 nm (when pH > 12), indicating that **1** may gradually dissociate to free $[Nb_6O_{19}]^{8-}$ and $[Ni(en)_3]^{2+}$ upon the addition of NaOH solution; this is further confirmed by the UV spectrum of $K_7HNb_6O_{19}$ (figure 6).

## 4. Conclusions

A new organic–inorganic hybrid polyoxoniobate based on Lindqvist-type anion and nickel complex has been synthesized using the diffusion strategy. The synthesis of **1** enriches the structural diversity of polyoxoniobates and provides a strategy for other transition-metal cations and organic ligands to construct polyoxoniobates and thus drive the quick development of the polyniobate chemistry.



## Supplementary material

Crystallographic data for the structural analysis reported in this article have been deposited with the Cambridge Crystallographic Data Centre with the deposited CCDC number [770256]. Copies of this information may be obtained free of charge from The Director, CCDC, 12 Union Road, Cambridge, CB2 1EZ, UK (Fax: +44-1223-336033; Email: deposit@ccdc.cam.ac.uk).

## Acknowledgments

This work was financially supported by the Natural Science Foundation of China, Special Research Fund for the Doctoral Program of Higher Education, Innovation Scientists and Technicians Troop Construction Projects of Henan Province, the Foundation of Education Department of Henan Province, and Natural Science Foundation of Henan Province.

## References

[1] M.T. Pope. *Heteropoly and Isopoly Oxometalates*, Springer-Verlag, Berlin (1983).
[2] M.T. Pope, A. Müller (Eds.). *Polyoxometalate Chemistry: From Topology Via Self-assembly to Applications*, Kluwer, Dordrecht (2001).

[3] I.V. Kozhevnikov. *Catalysts for Fine Chemical Synthesis–Catalysis by Polyoxometalates*, John Wiley and Sons, Chichester (2002).
[4] J.T. Rhule, C.L. Hill, D.A. Judd. *Chem. Rev.*, **98**, 327 (1998).
[5] C.M. Flynn, G.D. Stucky. *Inorg. Chem.*, **8**, 332 (1969).
[6] C.M. Flynn, G.D. Stucky. *Inorg. Chem.*, **8**, 335 (1969).
[7] E.J. Graeber, B. Morosin. *Acta Crystallogr., Sect. B*, **33**, 2137 (1977).
[8] T. Ozeki, T. Yamase, H. Naruke, Y. Sasaki. *Inorg. Chem.*, **33**, 409 (1994).
[9] H. Naruke, T. Yamase. *Acta Crystallogr., Sect. C*, **52**, 2655 (1996).
[10] H. Naruke, T. Yamase. *J. Alloys Comp.*, **255**, 183 (1997).
[11] A.V. Besserguenev, M.H. Dickman, M.T. Pope. *Inorg. Chem.*, **40**, 2582 (2001).
[12] M. Nyman, F. Bonhomme, T.M. Alam, M.A. Rodriguez, B.R. Cherry, J.L. Krumhansl, T.M. Nenoff, A.M. Sattler. *Science*, **297**, 996 (2002).
[13] M. Nyman, F. Bonhomme, T.M. Alam, J.B. Parise, G.M.B. Vaughan. *Angew. Chem. Int. Ed.*, **43**, 2787 (2004).
[14] F. Bonhomme, J.P. Larentzos, T.M. Alam, E.J. Maginn, M. Nyman. *Inorg. Chem.*, **44**, 1774 (2005).
[15] M. Nyman, A.J. Celestian, J.B. Parise, G.P. Holland, T.M. Alam. *Inorg. Chem.*, **45**, 1043 (2006).
[16] T.M. Anderson, T.M. Alam, M.A. Rodriguez, J.N. Bixler, W.Q. Xu, J.B. Parise, M. Nyman. *Inorg. Chem.*, **47**, 7834 (2008).
[17] R.P. Bontchev, M. Nyman. *Angew. Chem. Int. Ed.*, **45**, 6670 (2006).
[18] M. Maekawa, Y. Ozawa, A. Yagasaki. *Inorg. Chem.*, **45**, 9608 (2006).
[19] J.Y. Niu, P.T. Ma, H.Y. Niu, J. Li, J.W. Zhao, Y. Song, J.P. Wang. *Chem. Eur. J.*, **13**, 8739 (2007).
[20] R. Tsunashima, D.L. Long, H.N. Miras, D. Gabb, C.P. Pradeep, L. Cronin. *Angew. Chem. Int. Ed.*, **49**, 113 (2010).
[21] J.Y. Niu, G. Chen, J.W. Zhao, P.T. Ma, S.Z. Li, J.P. Wang, M.X. Li, Y. Bai, B.S. Ji. *Chem. Eur. J.*, **16**, 7082 (2010).
[22] R.P. Bontchev, E.L. Venturini, M. Nyman. *Inorg. Chem.*, **46**, 4483 (2007).
[23] L. Shen, C.H. Li, Y.N. Chi, C.W. Hu. *Inorg. Chem. Commun*, **11**, 992 (2008).
[24] J.P. Wang, H.Y. Niu, J.Y. Niu. *Inorg. Chem. Commun.*, **11**, 63 (2008).
[25] J.P. Wang, C.F. Yu, P.T. Ma, J.Y. Niu. *J. Coord. Chem.*, **62**, 2299 (2009).
[26] G. Chen, C.Z. Wang, P.T. Ma, J.P. Wang, J.Y. Niu. *J. Cluster Sci.*, **21**, 121 (2010).
[27] K. Hegetschweiler, R.C. Finn, R.S. Rarig Jr, J. Sander, S. Steinhauser, M. Wörle, J. Zubieta. *Inorg. Chim. Acta*, **337**, 39 (2002).
[28] M. Filowitz, R.K.C. Ho, W.G. Klemperer, W. Shum. *Inorg. Chem.*, **18**, 93 (1979).
[29] G.M. Sheldrick, *SHELXL-97, Program for Crystal Structure Solution*, University of Göttingen, Göttingen, Germany (1997).
[30] Y.B. Dong, M.D. Smith, H.C. Loye. *Inorg. Chem.*, **39**, 4927 (2000).
[31] Y. Gao, B. Twamley, J.M. Shreeve. *Organometallics*, **25**, 3364 (2006).
[32] S.Z. Li, J.W. Zhao, P.T. Ma, J. Du, J.Y. Niu, J.P. Wang. *Inorg. Chem.*, **48**, 9819 (2009).
[33] I. Lindqvist. *Ark. Kemi*, **5**, 247 (1953).
[34] I.D. Brown, D. Altermatt. *Acta Crystallogr., Sect. B*, **41**, 244 (1985).
[35] J.W. Zhao, B. Li, S.T. Zheng, G.Y. Yang. *Cryst. Growth Des.*, **7**, 2658 (2007).
[36] J.W. Zhao, S.T. Zheng, G.Y. Yang. *J. Solid State Chem.*, **180**, 3317 (2007).
[37] G.G. Gao, L. Xu, W.J. Wang, X.S. Qu, H. Liu, Y.Y. Yang. *Inorg. Chem.*, **47**, 2325 (2008).